AJNR

Computed tomography of carotid-cavernous fistula.

J Ahmadi, J S Teal, H D Segall, C S Zee, J S Han and T S Becker

AJNR Am J Neuroradiol 1983, 4 (2) 131-136
http://www.ajnr.org/content/4/2/131

Computed Tomography of Carotid-Cavernous Fistula

Jamshid Ahmadi[1]
James S. Teal[1,2]
Hervey D. Segall[1]
Chi-Shing Zee[1]
Jong-Suk Han[1,3]
Terry S. Becker[1]

Fourteen patients with angiographically-proven carotid-cavernous fistulas were evaluated by computed tomography (CT). Unilateral or bilateral exophthalmos was noted in 12 patients. Slight blurring of the margin of the globe was present in two, presumably due to pulsations of the globe or conjunctival edema. Superior ophthalmic veins were prominent in 12 patients and were often larger on the side of the fistula. Irregularity or absence of contrast enhancement of the superior ophthalmic vein may indicate partial or complete thrombosis. Focal bulging or diffuse distention of the cavernous sinus was noted in nine patients. Enlargement of the extraocular muscles was observed in seven with swelling of the eyelids and edema of the conjunctiva in eight patients. The pattern of venous drainage, type of fistula, and time intervals between trauma, commencement of fistula, and CT scan may affect the CT manifestations of carotid-cavernous fistulas.

Carotid-cavernous fistula is an uncommon disorder. Its dramatic ocular-orbital manifestations are principally due to altered regional hemodynamics and orbital venous hypertension. The eyes are at risk because of the potential development of ocular necrosis [1, 2].

The improved sensitivity and resolution of later generation computed tomographic (CT) scanners, due in part to finer beam collimation and matrices, have made it possible to evaluate orbital and sellar pathological processes in greater detail than with early generation scanners.

Only a few reports involving carotid-cavernous fistulas studied by CT have appeared [3, 4]. Sporadic cases also have been included in other papers dealing with CT evaluation of various types of intraorbital and parasellar pathology [5, 6]. The purpose of this communication is to report on the role, contributions, and reliability of CT in the evaluation of carotid-cavernous fistulas.

Subjects and Methods

Fourteen patients with carotid-cavernous fistulas were examined by CT. In all cases the fistulas were confirmed by cerebral angiography. There were seven men and seven women 26–65 years old. Direct internal carotid-cavernous sinus fistulas were present in 11 patients. In the other three patients, there were exclusively dural cavernous sinus malformations. In 12 patients, the fistulas were related to recent head injuries, while in the other two patients the fistulas occurred spontaneously. Fractures of the base of the skull were present in six patients.

In 11 patients CT was performed with an EMI 1010 dedicated head scanner using a scanning time of 80 sec and slices of 4 mm thickness with overlapping intervals of 2 mm between slices through the orbital and parasellar regions. These scans were obtained only in the axial plane. In the other three patients, axial and coronal CT scans were obtained with a General Electric CT/T8800 scanner using adjacent 5 mm slices without overlapping, and a scanning time of 9.6 sec. All CT scans were obtained before and after intravenous infusion of iodinated contrast medium (Reno-M-Dip, 42 g iodine/300 ml solution). A summary of clinical features is present on table 1.

Received November 13, 1981; accepted after revision September 15, 1982.

[1]Department of Radiology, University of Southern California School of Medicine, LAC-USC Medical Center, Box 2, 1200 N. State St., Los Angeles, Ca 90033. Address reprint requests to J. Ahmadi.

[2]Present address: Department of Radiology, Howard University Medical Center, Washington, DC 20001.

[3]Present address: Department of Radiology, Case Western Reserve Medical Center, Cleveland, OH 44106.

AJNR 4:131–136, March/April 1983
0195-6108/83/0402-0131 $00.00

TABLE 1: **Summary of Clinical Observations in Carotid-Cavernous Fistulas**

Type of Fistula: Case No. (age, gender)	Clinical Aspects
Internal carotid:	
1 (58, F)	Head trauma 2½ weeks before second CT. Proptosis, chemosis R eye. First CT 1 day after trauma was normal. No clinical symptoms of CCF at initial CT.
2 (45, M)	Fist fight 2½ months before CT. Headache, bruit.
3 (60, F)	Auto accident, loss of consciousness 2 months prior to CT scan. L proptosis and ophthalmoplegia.
4 (28, M)	Auto accident 1 day before first CT which only showed facial fx. He later developed proptosis, chemosis, and bruit. Second CT 3 months after head trauma.
5 (65, F)	L orbital proptosis 5 months before CT.
6 (44, F)	Auto accident 5 weeks before CT. Bilateral proptosis.
7 (32, F)	Head trauma 3 weeks before CT.
8 (26, M)	Gunshot wound 2 weeks before CT.
9 (25, M)	Gunshot wound and R hemiparesis 2 days before normal first CT. Proptosis developed 10 days later. Second CT then performed.
10 (36, M)	Gunshot wound 2 days before CT. Proptosis, chemosis, and blindness L eye.
11 (23, M)	Auto accident 2 months before CT.
Dural:	
12 (63, M)	Proptosis, chemosis, and whooshing noise in head 8 months prior to CT.
13 (33, F)	Auto accident 3 months before CT. Proptosis and reduced visual acuity L eye.
14 (46, F)	Head trauma 3 weeks before CT. Proptosis and noise in head.

Note.—R = right; L = left; CCF = carotid-cavernous fistula; fx = fracture.

A series of 160 normal axial CT scans was used as a baseline for comparison. These scans were selected from a larger series initially performed on the EMI-1010 on patients with galactorrhea and/or elevated serum prolactin suspected of having pituitary microadenomas and had been interpreted as normal by two neuroradiologists. Only those scans were selected that provided adequate sections of 4 mm thickness with overlap through the orbital and parasellar regions, including a section through the apex of the orbit and lens in the same plane, with the globe in the neutral gaze looking straight forward to minimize alteration of measurements of globe shifts.

A method for determining the position of the globe in relation to the bony orbit was devised. A line was drawn between the most anteromedial portion of the zygomatic process to the angle formed at the junction of the nasal bone and the most anterior part of the medial orbit (constructed zygomatic line, or CZL). The shortest distance from this constructed line to the anterior margin of each globe was measured. These measurements were made using an orbital CT section that included the lens and orbital apex in the same plane so as to avoid inconsistency (fig. 1). The advantage of this line over the interzygomatic line, employed by Hilal et al. [6], is that this line can be used even if the head is slightly tilted.

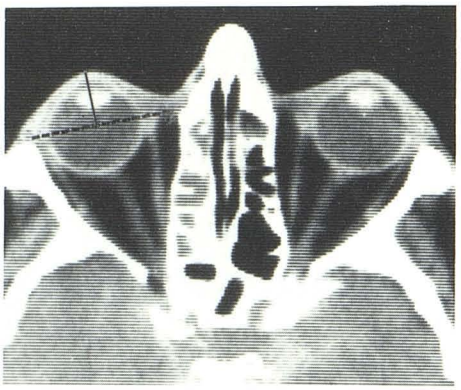

Fig. 1.—Method for determining position of globe relative to bony orbit. Line is constructed from most anterior part of zygomatic process to angle formed at junction of nasal bone and most anterior part of medial orbital wall (*broken line*). Normally, about one-half of the greatest anteroposterior diameter of the globe is projected in front of this line.

TABLE 2: **Normal Dimensions in 160 Orbital CT Scans**

	Range (mm)
Greatest thickness of medial or lateral rectus muscles in each orbit	3–4
Maximum diameter of superior ophthalmic vein	2–3.5
Distance from anterior margin of globe to constructed zygomatic line	11–13
Greatest anteroposterior diameter of globe	24–27

The greatest thickness of the larger of the medial or lateral rectus muscles in each orbit was measured and recorded. The maximum diameter of each superior ophthalmic vein was also measured and recorded. The normal range of these anatomic parameters is charted in table 2. All measurements recorded are actual measurements, corrected for minification.

Results

In the control group, 11–13 mm of the globe projected anterior to the CZL. The mean value was 12 mm (2 SD = ±1.5 mm). This corresponds to a mean percentage of 46.7% (2 SD = ± 5.5%) of the greatest anteroposterior diameter of the globe. Since gaze shifts may alter the position of the globe, such shifts may also minimally after this measurement. Exophthalmos was considered to be present if more than 52% of the globe projected anterior to the CZL; on this basis, exophthalmos was present in 12 of 14 patients. It was severe (distance from CZL to anterior margin of globe ≥ 20 mm, i.e., 80% exophthalmos) in five; moderate (17–19 mm, i.e., 68%–78%) in six; and mild (14–16 mm, i.e., 56%–64%) in one case. In four patients the exophthalmos was bilateral. Slight blurring of the margin of

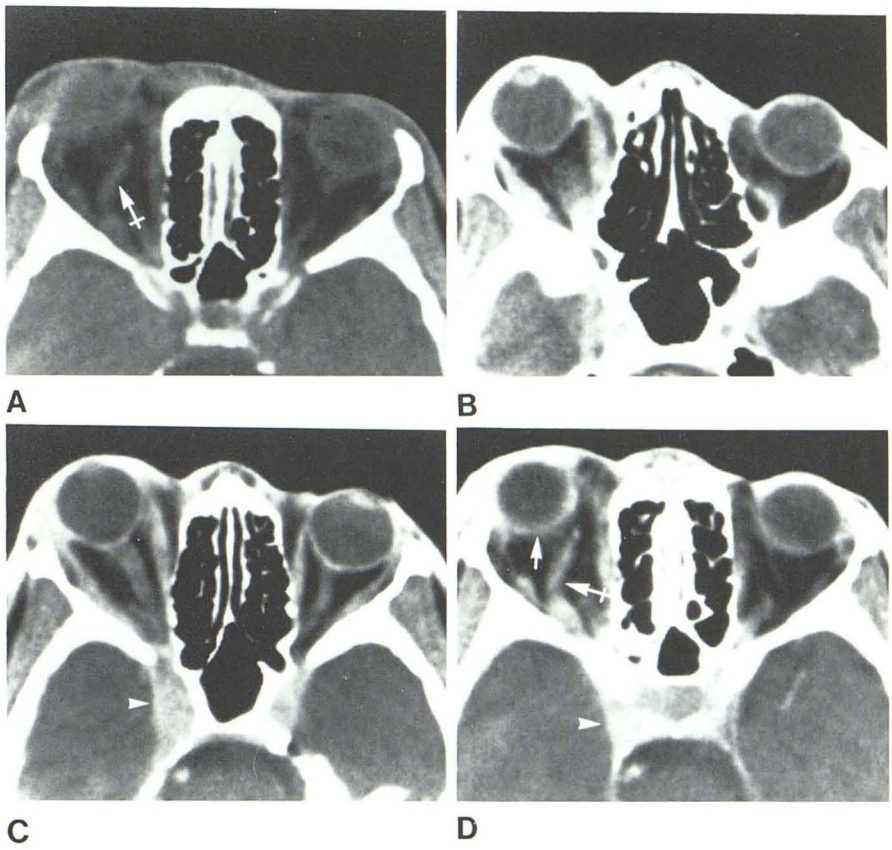

Fig. 2.—Case 1, right internal carotid-cavernous fistula. Precontrast (**A**) and postcontrast (**B–D**) CT. Marked proptosis, dilatation of superior ophthalmic vein (*crossed arrow*), enlargement of extraocular muscles, and distention of cavernous sinus on right side (*arrowhead*). Blurring of margin of globe in **D** is presumably due to pulsations of globe or conjuntival edema (*arrow*).

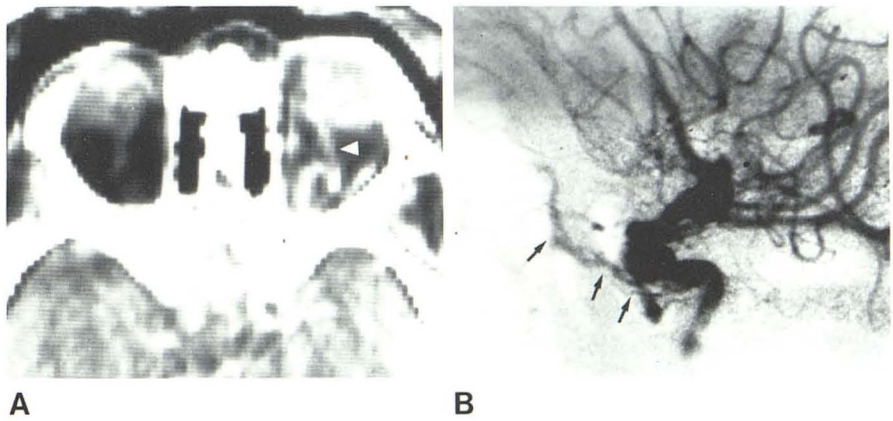

Fig. 3.—Case 5, spontaneous left internal carotid-cavernous fistula with partial thrombosis. **A**, Postcontrast axial CT scan. Left proptosis, periorbital swelling, enlargment of extraocular muscle, dilatation and kinking of superior ophthalmic vein (*arrowhead*). **B**, Left internal carotid arteriogram. Slow opacification and irregular filling defects of left superior ophthalmic vein and cavernous sinus (*arrows*). Arteriosclerotic changes of cavernous and supraclinoid segments of internal carotid artery are evident.

the globe could be appreciated in two patients, presumably due to pulsations of the globe or conjunctival edema (fig. 2).

The superior ophthalmic vein is the largest intraorbital vein. We were able to identify at least a part of this vein in 46% of normal orbital CT scans. Frequently the second and third segments of the superior ophthalmic vein were visualized as an obliquely oriented tubular structure in the CT section above the optic nerve. There was considerable variation of the diameter in normal subjects. Its maximum diameter, however, did not exceed 3.5 mm in the normal group.

Dilatation of the superior ophthalmic vein was noted in 12 patients. The vein on the affected side was often larger than on the opposite side. The degree of distention appeared to be affected by the hemodynamics and the pattern of venous drainage. Partial or complete thrombosis was observed angiographically in two patients. Contrary to previous re-

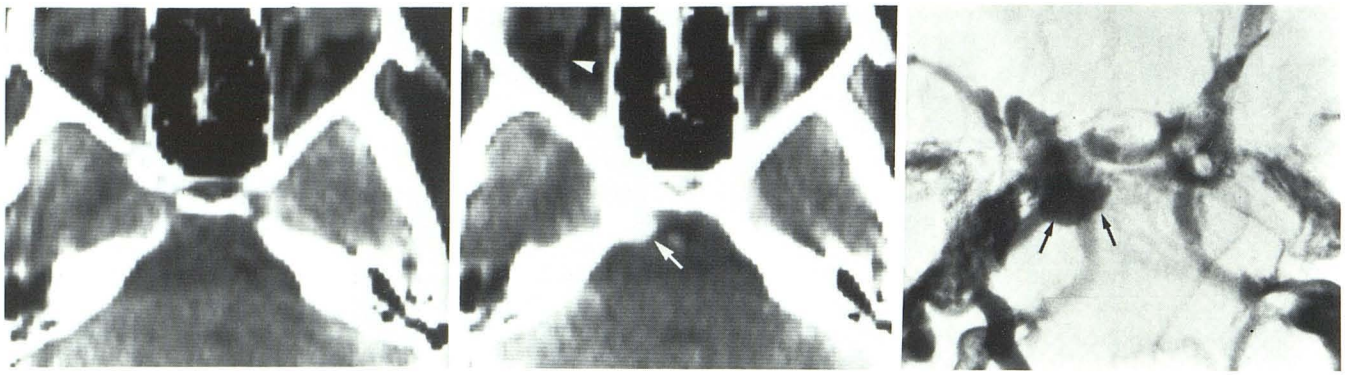

Fig. 4.—Case 6, traumatic internal carotid-cavernous sinus fistula and thrombosis of right superior ophthalmic vein. Precontrast (**A**) and postcontrast (**B**) axial CT scans. Focal distention of posterolateral part of affected side of cavernous sinus (*arrow*). Absence of contrast enhancement of slightly prominent superior ophthalmic vein on affected side (*arrowhead*), while prominent superior ophthalmic vein on opposite side of fistula enhances markedly. **C**, Selective right internal carotid arteriogram, submentovertex projection. Immediate shunting from internal carotid artery into right cavernous sinus resulting in focal distention of cavernous sinus. No filling of right superior ophthalmic vein with good filling of left superior ophthalmic vein.

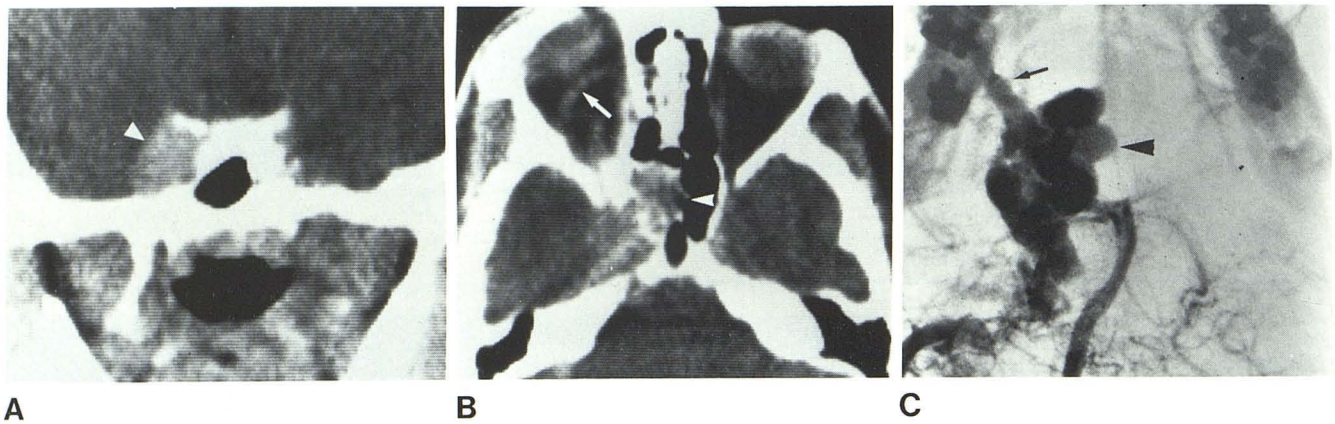

Fig. 5.—Case 11, traumatic carotid-cavernous fistula. Coronal (**A**) and axial (**B**) contrast-enhanced CT scans. Markedly expanded right cavernous sinus has resulted in destruction of adjacent osseous wall of sphenoid sinus, filling right half of sinus (*arrowheads*). Slightly prominent right superior ophthalmic vein (*arrow*) aids in differential diagnosis of fistula from other expanding lesions of cavernous sinus region with similar CT appearance. **C**, Right vertebral arteriogram, submentovertex projection. CT appearance correlates accurately with arteriogram.

ports [3, 7], contrast enhancement of the superior ophthalmic vein was noted in both normal and carotid-cavernous fistula groups. Kinking of the vein may indicate partial (fig. 3) and absence of the vein complete (fig. 4) thrombosis [8].

Normal cavernous sinues are paired, roughly quadrangular structures in the transverse plane, lying adjacent to each lateral margin of the sella turcica. In the control group, the lateral margin of the normal cavernous sinus was noted to be either straight or slightly concave [9]. Abnormal shape and size of the contrast-enhanced cavernous sinus was noted in nine patients with fistulas. Three cases showed focal distention of the lateral wall of the cavernous sinus (fig. 4). Diffuse bilateral or unilateral expansion of the cavernous sinus was noted in six patients (fig. 5). Distention of the sinus was more prominent on the side of the fistula.

Enlargement of the extraocular muscles was observed in seven cases of carotid-cavernous fistulas. The normal range of extraocular muscle thickness was 3–4 mm. Swelling of the eyelids and edema of the conjunctiva were noted in eight patients. None of the patients demonstrated CT evidence of cerebral ischemia.

Discussion

The cavernous sinus is a duroperiosteal space, containing a trabeculated network of venous channels surrounding the juxtasellar segment of the internal carotid artery and its dural branches [10]. Spontaneous or traumatic rupture of the wall of the intracavernous segment of the carotid artery or its dural branches results in sudden shunting of the arterial blood into the cavernous sinus and thence into the orbital veins and other venous connections. There is a rich venous network in the orbit. These venous channels are

without valves and drain into the cavernous sinus. Under the continuous load shunted of arterial blood, these veins dilate tremendously and their media thicken considerably [11]. The superior ophthalmic vein is the major intraorbital vein and interconnects with all other intraorbital veins.

The diameter of the superior ophthalmic vein varies considerably in normal individuals. Its normal range at orbital phlebography has been reported to vary from 0.8–4.8 mm when no venous compression is applied [12]. However, even in the absence of venous compression, distention of the superior ophthalmic vein is possible during orbital phlebography due to the pressure of the injection. In this and other normal series [7], the diameter of the vein seen by CT was 2–3.5 mm. Tortuosity and dilatation of the vein are the hallmarks of carotid-cavernous fistulas; however, these signs may be associated with a variety of other conditions such as orbital venous malformation and varices, angiomas, vascular tumors, dysthyroid ophthalmopathy, and occlusion or thrombosis of the superior ophthalmic vein [13–15].

Focal bulging or distention of the cavernous sinus in carotid-cavernous fistula is the result of altered hemodynamics. If in the presence of fistula the intercommunicating venous channels are large enough to allow free flow to blood into the opposite side, both cavernous sinuses may expand and both eyes may become involved. A tortuous cavernous portion of the internal carotid artery [16], intracaverous carotid artery aneurysms, pituitary adenoma extending into the cavernous sinus, and primary metastatic neoplasm involving the cavernous sinus [17] may also result in apparent distention of the cavernous sinus. However, such an area of distention or bulge in a patient with a huge high-flow fistula does not necessarily imply an aneurysm in association with the fistula.

Enlargement of extraocular muscles is primarily due to congestion and edema of the intraorbital soft tissues. It is a nonspecific feature, and may be seen in a number of conditions such as orbital inflammation [18], trauma, and particularly Graves ophthalmopathy [15].

Several factors alone or in combination may affect the CT manifestations of carotid-cavernous fistula: (1) time interval between trauma, commencement of fistula, and CT scan; (2) pattern of venous drainage; and (3) type of fistula. Since there is usually a delay between the traumatic incident and the clinical manifestation of carotid-cavernous fistula, it is likely that development of the fistula is either slow or delayed. This would account for the usual paucity of CT findings noted within the first few days after head trauma (cases 1, 4, and 9). Excellent correlation between CT and angiography was noted with respect to the pattern of venous drainage (fig. 4). The degree of exophthalmos was more closely related to the size of the superior ophthalmic vein than to the other parameters evaluated. Carotid-cavernous fistulas located in the anterior aspect of the cavernous sinus tended to drain predominently into the superior ophthalmic vein. The degree of exophthalmos tended to be somewhat less with dural malformations than with true internal carotid-cavernous fistulas.

The dramatic ocular-orbital symptoms are principally due to increased pressure within the orbital venous system. Orbital venous hypertension causes congestion and edema of the intraorbital tissues. In most instances, the clinical picture of pulsating exophthalmos and chemosis with a distressing persistent bruit in the head is so striking that a confident diagnosis of carotid-cavernous fistula is made on the basis of the clinical manifestations alone. Selective cerebral angiography then confirms the diagnosis and furnishes the detail of the circulatory status. Occasionally, however, only part of the symptom complex is manifested, such as proptosis without bruit, presenting a diagnostic problem from a clinical standpoint [19]. CT may play a useful role in the evaluation of unilateral or bilateral exophthalmos [20]. When the superior ophthalmic vein is noted to be prominent, with focal bulging or distention of the cavernous sinus, carotid-cavernous sinus fistula must be considered. However, the definitive diagnostic test is angiography. A baseline CT scan before any treatment of the carotid cavernous fistula may be helpful furthermore to distinguish posttraumatic sequelae from complications occurring after treatment.

REFERENCES

1. Sanders MD, Hoyt WF. Hypoxic ocular sequelae of carotid-cavernous fistulae. *Br J Ophthalmol* **1969**;53:82–97
2. Spencer WH, Thompson HS, Hoyt WF. Ischemic ocular necrosis from carotid-cavernous fistula, pathology of stagnant anoxic inflammation of orbital and ocular tissue. *Br J Ophthalmol* **1973**;57:145
3. Merrick R, Latchaw RE, Gold LH. Computerized tomography of the orbit in carotid-cavernous sinus fistulas. *Comput Tomogr* **1980**;4:127–132
4. Zilkha A, Diaz AS. Computed tomography in carotid-cavernous fistula. *Surg Neurol* **1980**;14:325–329
5. Hilal SK, Trokel SL. Computerized tomography of the orbit using thin sections. *Semin Roentgenol* **1977**;12:137–147
6. Moseley IF, Sanders MD, Claveria LE. Diagnostic limitations of computerized tomographic examination of the orbit. In: Bories J, ed. *The diagnostic limitation of computerized axial tomography*. New York: Springer-Verlag, **1976**:52–62
7. Bacon KT, Duchesneau PM, Weinstein MA. Demonstration of the superior ophthalmic vein by high resolution computed tomography. *Radiology* **1977**;124:129–131
8. Seeger JF, Gabrielsen TO, Giannotta SL, Lotz PR. Carotid-cavernous sinus fistulas and venous thrombosis. *AJNR* **1980**;1:141–148
9. Segall HD, Ahmadi, J, McComb JG, Zee CS; Becker TS, Han JS. Computed tomographic observations pertinent to intracranial venous thrombotic and occlusive disease in childhood. State of the art, some new data, and hypotheses. *Radiology* **1982**;143:441–449
10. Parkinson, D. Anatomy of the cavernous sinus. In: Smith JL, ed. *Neuro-ophthalmogy*. Symposium of the University of Miami and the Bascom Palmer Eye Institute. St. Louis: Mosby, **1972**:73–101
11. Hamby WB. **Carotid-cavernous fistula**. Springfield, IL: Thomas, **1966**:36
12. Brismar J. Orbital phlebography II. Anatomy of superior ophthalmic vein and its tributaries. *Acta Radiol* [*Diagn*](Stock) **1974**;15:481–496
13. Doyon DL, Aron-Rosa DS, Ramee A. Orbital views & cavernous sinus. In: Newton TH, Potts DG, eds. *Radiology of the skull and brain*. St. Louis: Mosby, **1974**:2221–2254

14. Glyn AS, Lloyd DM. Pathological veins in the orbit *Br J Radiol* **1974**;47:570–578
15. Enzmann D, Marshall WH Jr, Rosenthal AR, Kriss JP. Computed tomography in Grave's ophthalmopathy. *Radiology* **1976**;118:615–620
16. Hayman LA, Evans, RA, Hinck VC, Rapid high dose (RHD) contrast computed tomography of perisellar vessels. *Radiology* **1979**;131:121–123
17. Kline LB, Acker JD, Post MJD, et al. The cavernous sinus. A computed tomographic study. *AJNR* **1982**;2:299–305
18. Enzmann D, Donnalson SS, Marshall WH, Kriss JP. Computed tomography in orbital pseudotumor (idiopathic orbital inflammatory). *Radiology* **1976**;120:597–601
19. Taniguchi RM, Gorre JA, Odom GL. Spontaneous carotid-cavernous shunts presenting diagnostic problems. *J Neurosurg* **1971**;1:81–100
20. Salvolini U, Menichelli F, Pasquini U. Computed assisted tomography in 90 cases of exophthalmos. *J Comput Assist Tomogr* **1977**;1:81–100